

Research Article

Open Access

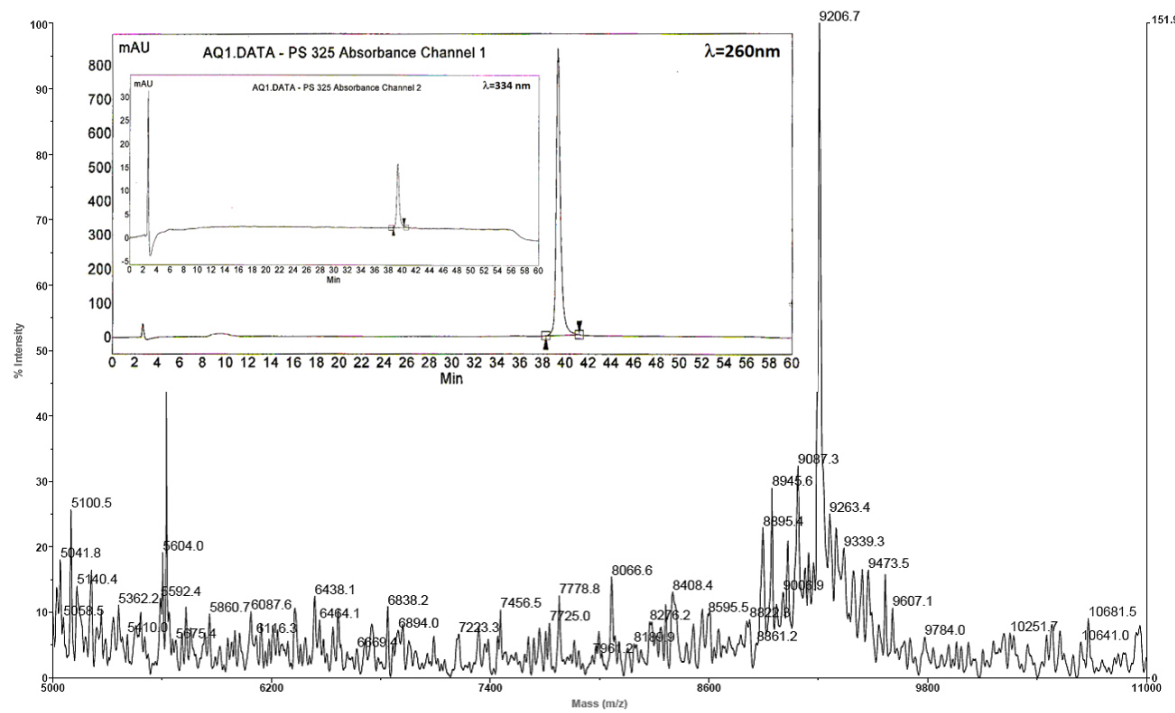
Boleslaw T. Karwowski

Supplement: The influence of the phosphorothioate diester bond on the DNA oxidation process

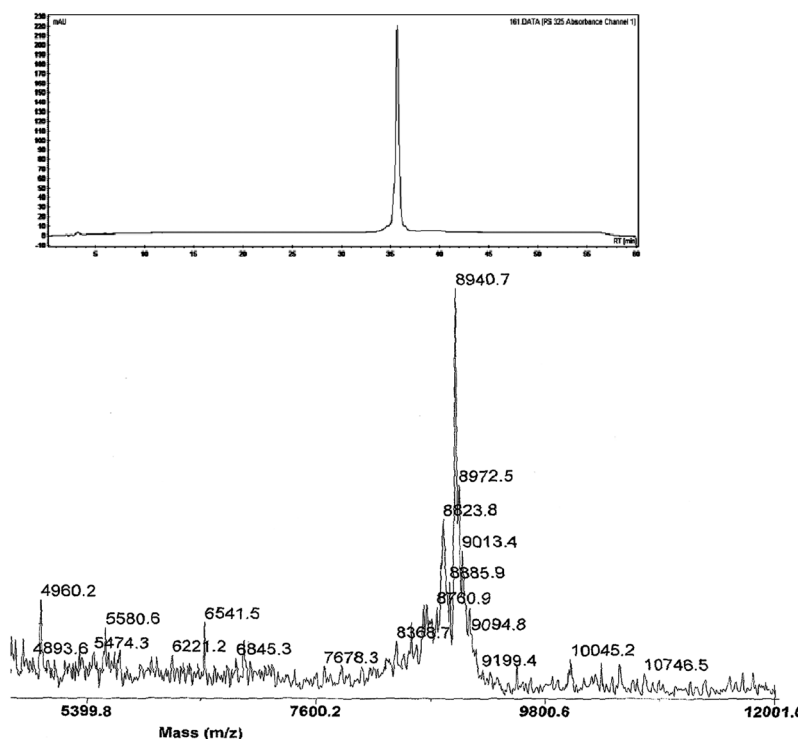
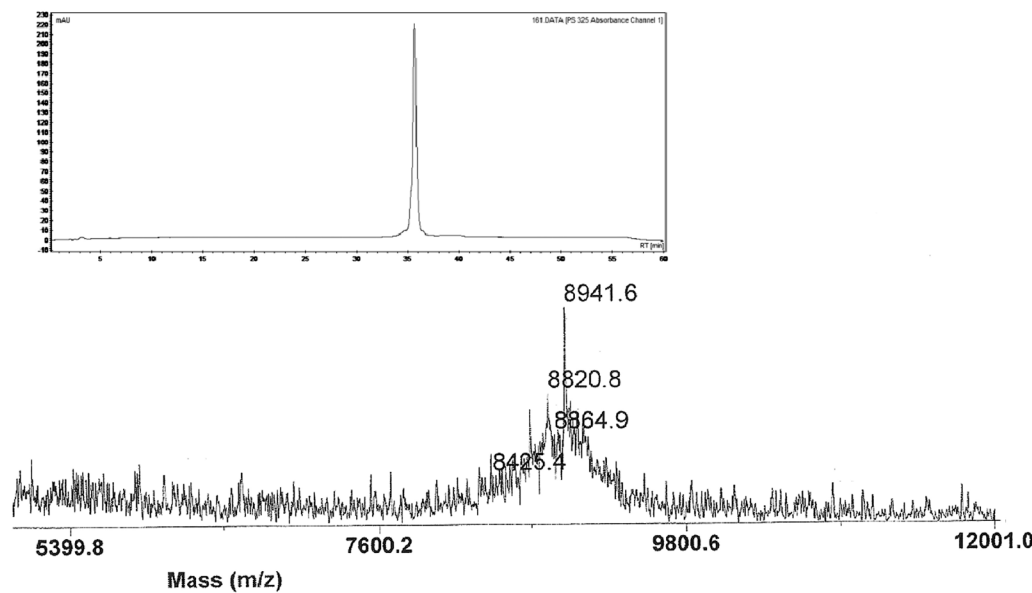
Supplementary Table 1: Sequence of investigated oligonucleotides and results of their MALDI-TOF analysis.

	Oligonucleotide Sequence	CalculatedMass	ObtainedMass
A	5'-AAATTAATAT _{ps} G TATTGTATATAAATTATT-3'	8943	8941
B	5'-AAATTAATAT G _{ps} TATTGTATATAAATTATT-3'	8943	8942
C	5'-AAATTAATAT G TATT _{ps} T ATATAAATTATT-3'	8943	8947
D	5'-AAATTAATAT _{ps} G TATT _{ps} T ATATAAATTATT-3'	8959	8960
E	5'-AAATTAATAT G TATTGTATATAAATTATT-3'	8927	8927
F	3'-TTTAATTATACATAACATATATTAAATAA-5'	8856	8960
AQ-PO-29	3'-TTTAATTATACATAACATATATTAAATAA-PO-AQ-5'	9215	9207

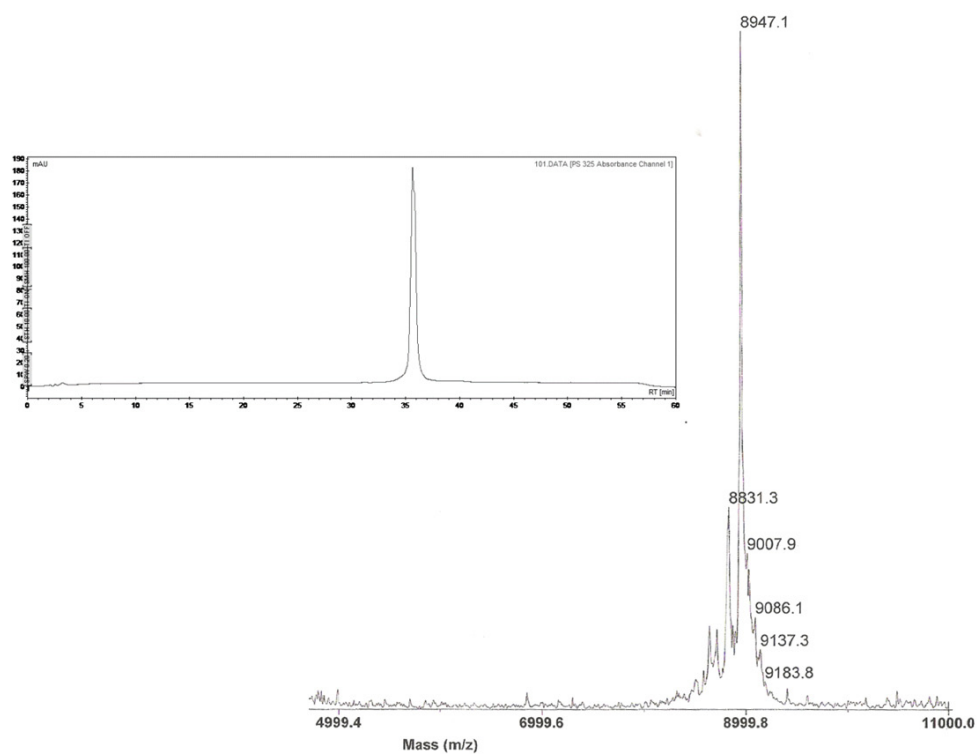
MALDI-TOF spectra and RP-HPLC profile of **Oligodeoxynucleotide AQ-PO-29** at λ -260 nm and λ -334 nm detection.



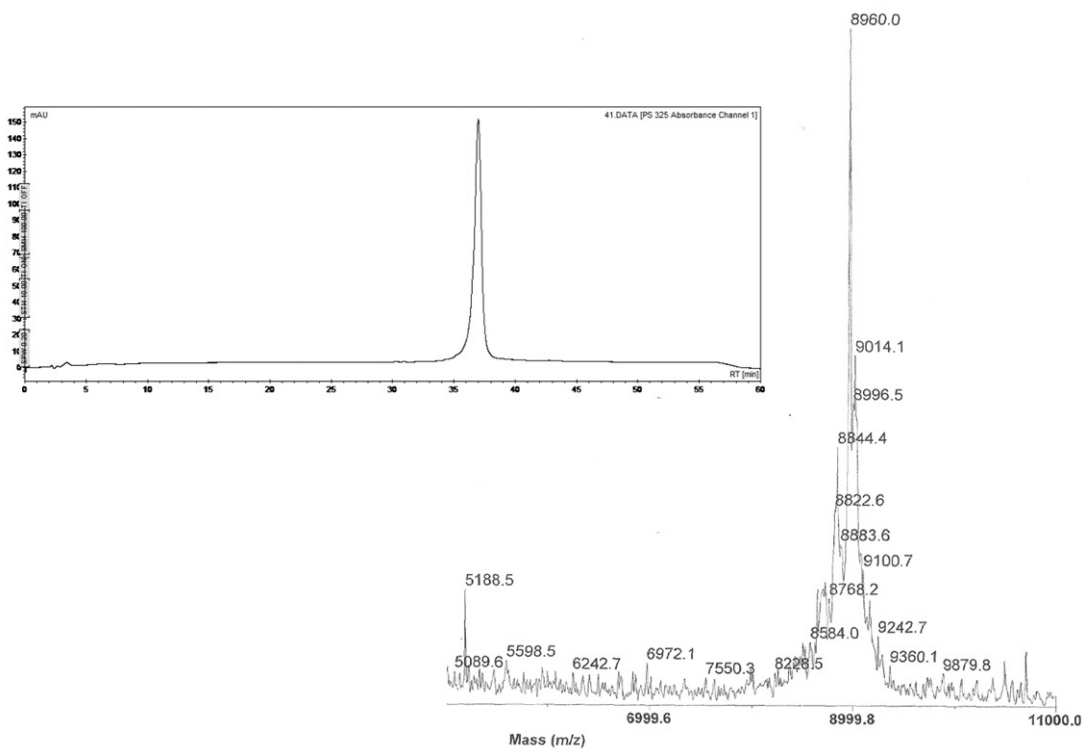
***Corresponding author:** Boleslaw T. Karwowski: Food Science Department , Medical University of Lodz, ul. Muszynskiego 1, 90-151 Lodz, Poland, E-mail: Bolek.Karwowski@wp.pl

MALDI-TOF spectra of Oligodeoxynucleotide A and RP-HPLC profile at λ -260 nm detectionMALDI-TOF spectra of Oligodeoxynucleotide B and RP-HPLC profile at λ -260 nm detection

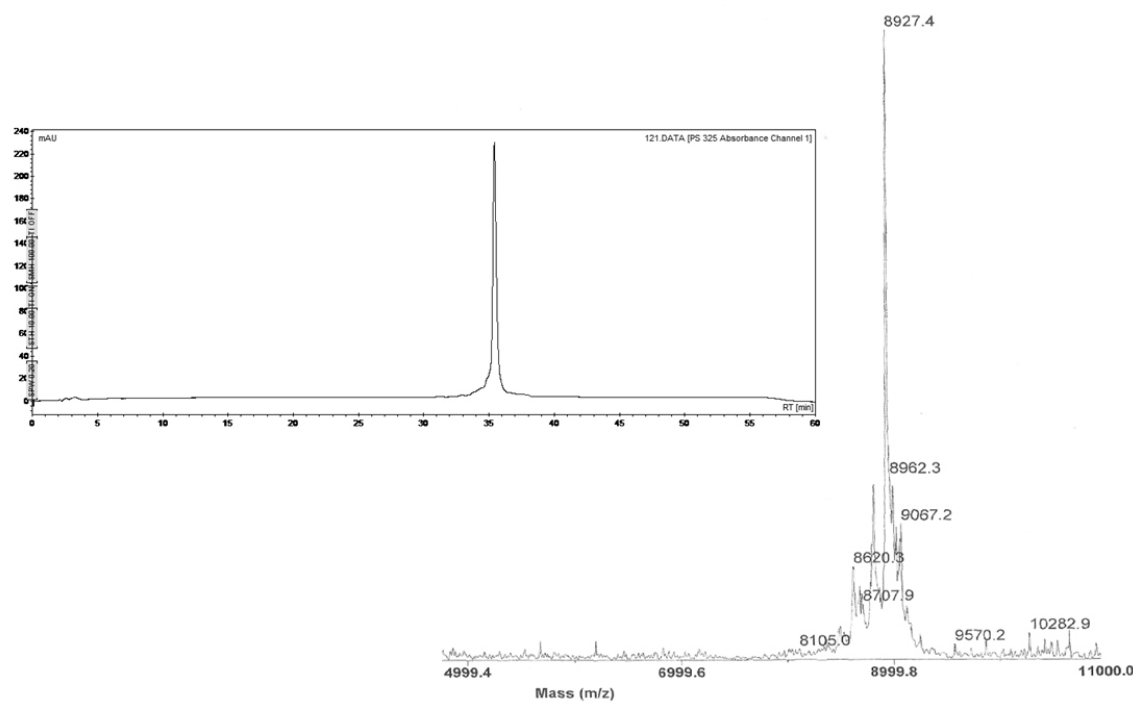
MALDI-TOF spectra of Oligodeoxynucleotide C and RP-HPLC profile at λ -260 nm detection.



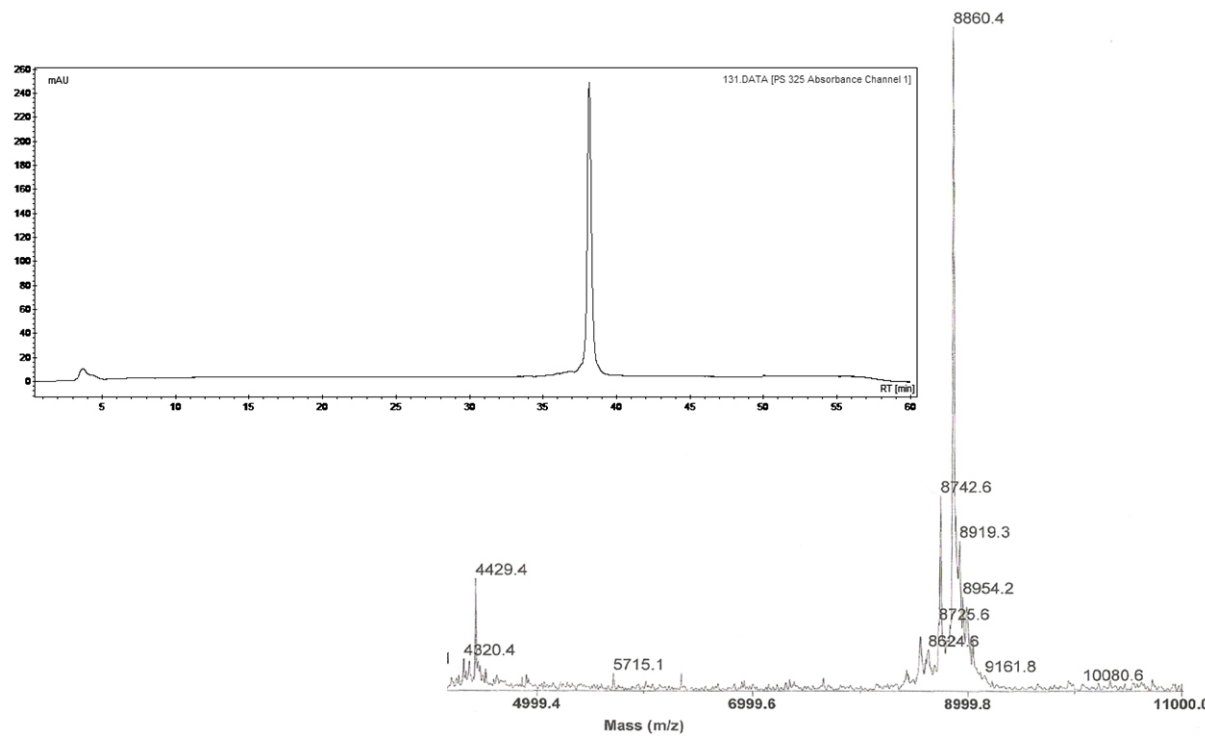
MALDI-TOF spectra of Oligodeoxynucleotide D and RP-HPLC profile at λ -260 nm detection.



MALDI-TOF spectra of Oligodeoxynucleotide E and RP-HPLC profile at λ -260 nm detection.

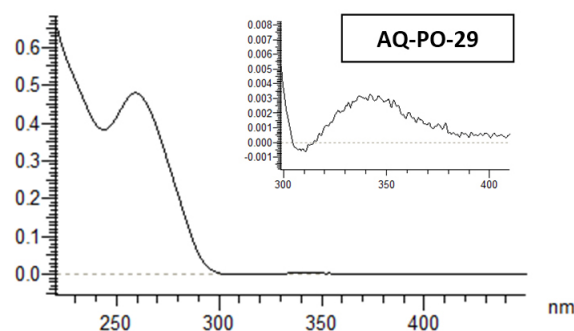


MALDI-TOF spectra of Oligodeoxynucleotide F and RP-HPLC profile at λ -260 nm detection.



Determination of Oligonucleotide Concentration

The concentration of the obtained oligonucleotides was determined from a maximum of absorbance ~ 260 nm using a Hitachi U-2800 spectrophotometer. The online oligonucleotide properties calculator (OligoCalc) was used to determine the oligonucleotide extinction coefficient; in the case of AQ-PO-29, adenine was used instead of an anthraquinone moiety (Gasper, M.S. and G.B. Shuster (1997). Intramolecular Photoinduced Electron Transfer to Anthraquinones Linked to Duplex DNA: The Effect of Gaps and Traps on Long-Range Radical Cation Migration. *J. Am. Chem. Soc.* **119**, 12762-12771).



Supplementary Figure 1: UV/VIS spectra of oligonucleotide containing antraquinone moiety AQ-PO-29

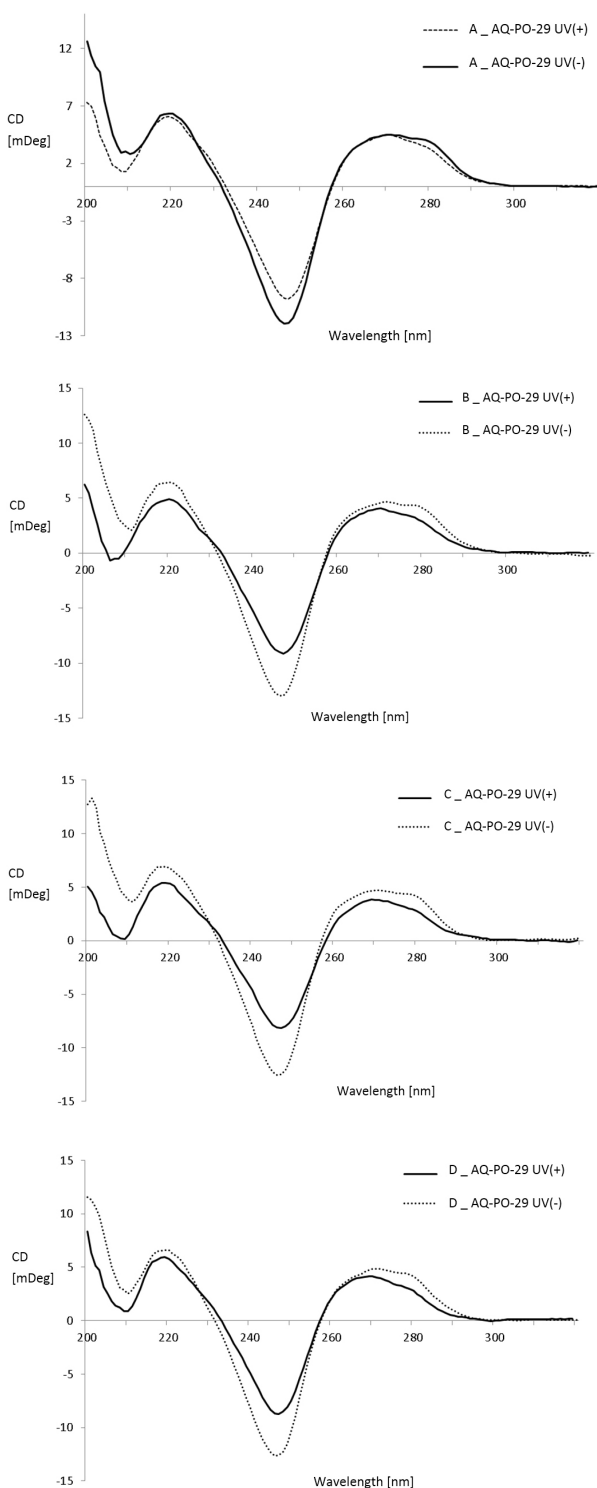
Oligonucleotide thermal stability, i.e. melting temperature measurement

Supplementary Table 2: Melting temperatures, as a maximum of first derivatives, obtained for double-stranded oligonucleotides.

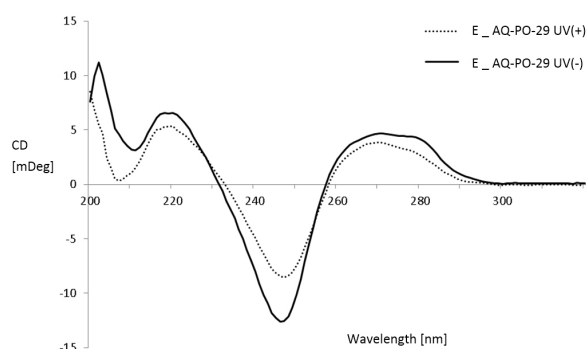
ds-DNA	Tm [°C]	
	AQ(+)*	AQ(-)
A	55.39	52.32
B	55.30	52.19
C	54.65	51.35
D	50.25	43.40
E	58.64	53.33
H	-----	53.33

* The AQ(+) complementary strand contains an anthraquinone unit (AQ-PO-29); the AQ(-) complementary strand is without an anthraquinone unit (oligonucleotide F).

Oligonucleotide circular dichroism analysis

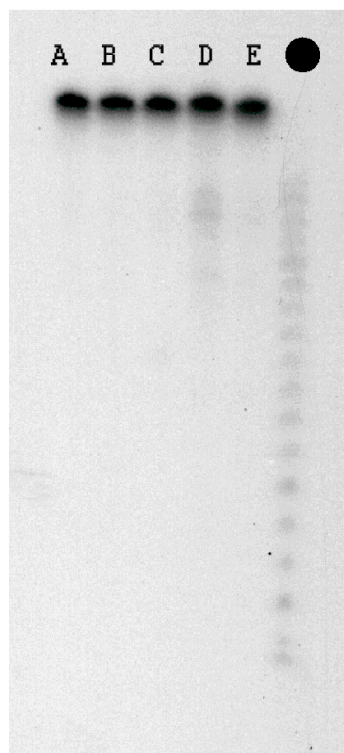


Supplementary Figure 2: Circular dichroism spectra of investigated oligonucleotides. UV (+) indicated that the sample was previously irradiated by 350 nm light for 120 min, UV (-) dark sample.



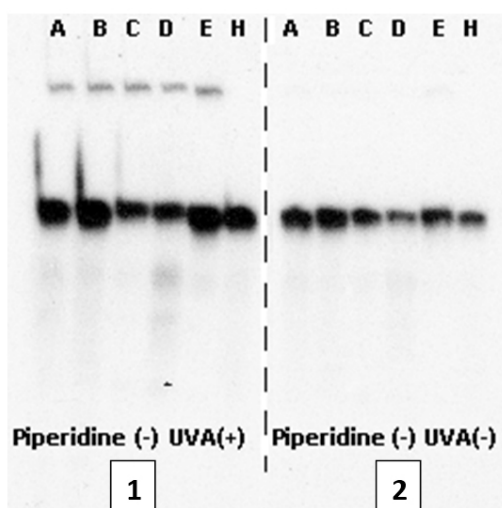
Supplementary Figure 2: Circular dichroism spectra of investigated oligonucleotides. UV (+) indicated that the sample was previously irradiated by 350 nm light for 120 min, UV (-) dark sample.

Autoradiogram of purified and 5'-end ^{32}P Labelled Oligonucleotides used.

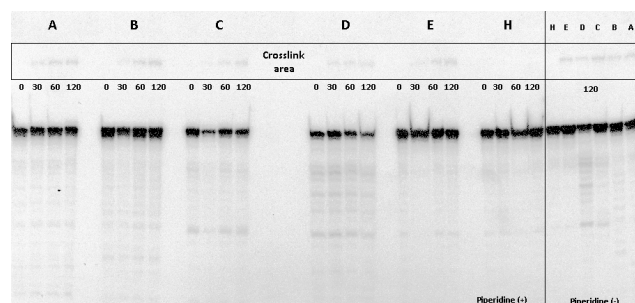


Supplementary Figure 3: Autoradiogram showing the purity of the investigated oligonucleotide. (Denaturing 7M urea 20% polyacrylamide gel electrophoresis) Line A-E oligonucleotide (the sequence of which is given in Table 1SM).

ds-DNA cleavage analysis after UVA irradiation.



Supplementary Figure 4a: Autoradiogram of irradiated (1) and un-irradiated (2) ds-DNA after: 120 minutes without piperidine treatment. (Denaturing 7M urea 20% polyacrylamide gel electrophoresis.) The line A-H oligonucleotide corresponding to double-stranded oligonucleotides is described in the main text of the article.



Supplementary Figure 4b: Autoradiogram of the results of irradiation of AQ-linked ds-DNAs: A–H, in the presence of superoxide dismutase (SOD) and oxygen, after (+) and before (-) piperidine treatment. Radiation time is given in minutes.

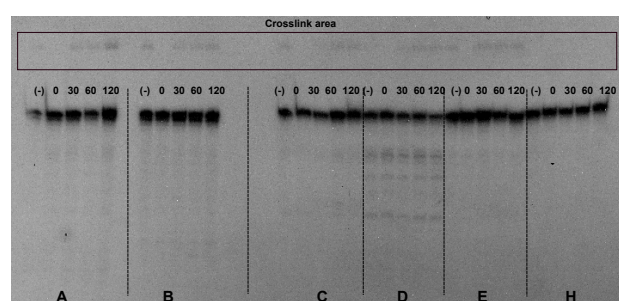
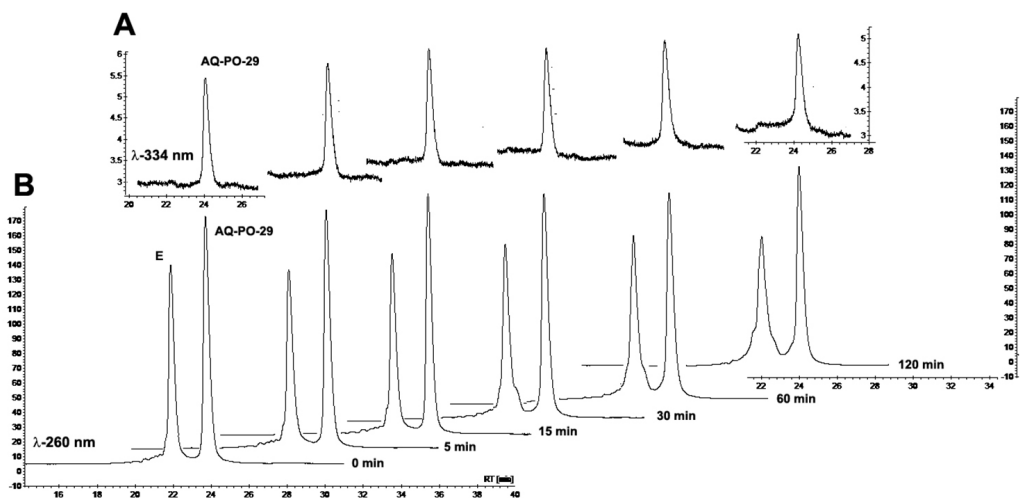
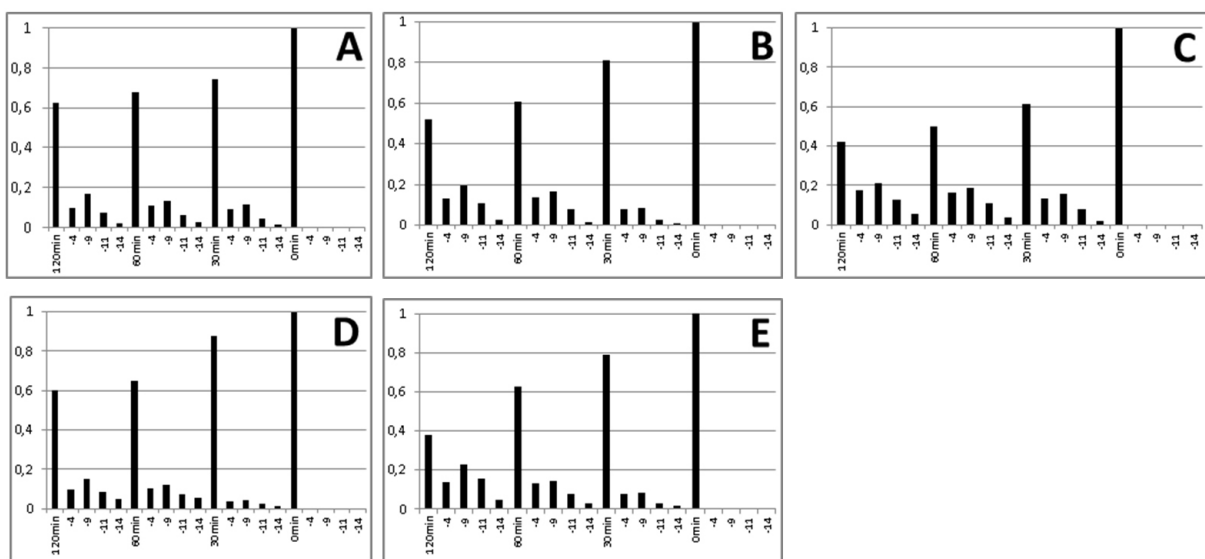


Figura 4cSM. Autoradiogram of the results of irradiation of AQ-linked ds-DNAs: A–E, in the absence of oxygen, after and before (track (-), 120 min of irradiation) piperidine treatment. Irradiation time is given in minutes.

**RP-HPLC chromatogram profiles of ds-DNA after UVA
(λ -350 nm) irradiation**

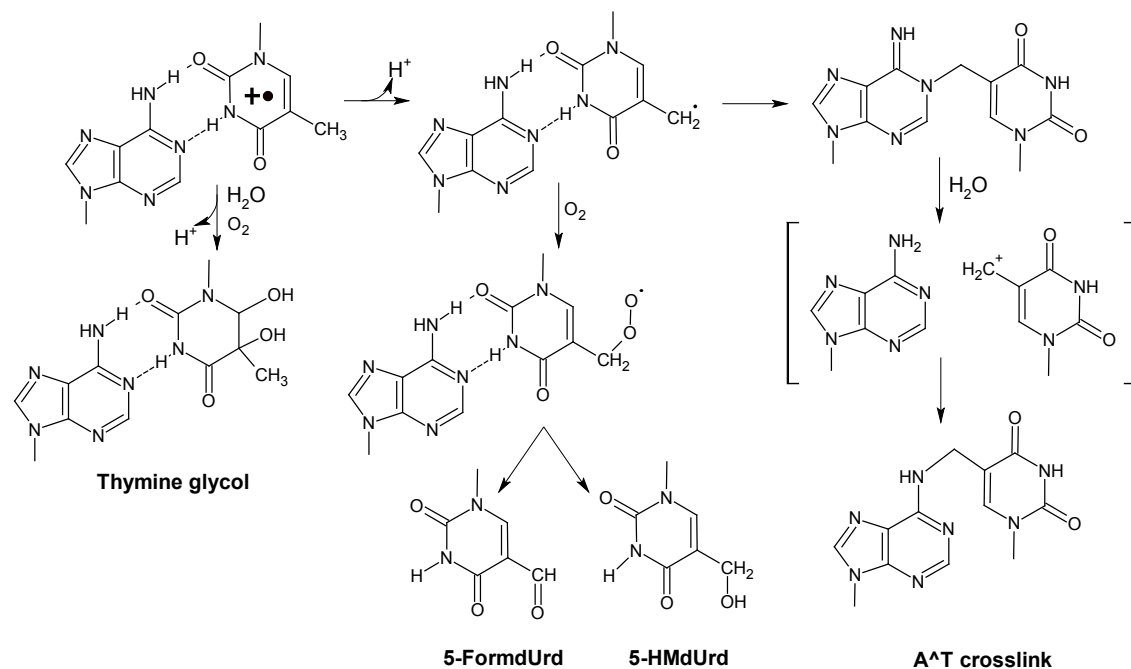


Supplementary Figure 5: RP-HPLC analysis (detection A: λ -334 nm, B: λ -260 nm) of the double-stranded oligonucleotides, i.e. oligo-E/AQ-PO-29 stability after 0, 15, 30, 60, 120 min of UVA irradiation.



Supplementary Figure 6: Cleavage efficiency given in [%] of the investigated double-stranded oligonucleotides. The corresponding autoradiograms are given in the main the body of article (Fig. 3). Irradiation time 0, 30, 60, 120 minutes, -4 corresponding to T26, -9 to T21, -11 to T19, -14 to G19 in the sequence of ^{32}P radiolabelled strand.

Double-stranded oligonucleotides					
Irradiation time	A	B	C	D	E
120 min	0.624537	0.520314	0.421358	0.599859	0.381469
-4 (T26)	0.095107	0.13286	0.177238	0.098764	0.14037
-9 (T21)	0.169525	0.195963	0.212826	0.148312	0.227552
-11 (T19)	0.073504	0.108899	0.126533	0.087592	0.157571
-14 G19)	0.020442	0.024713	0.056198	0.04718	0.049206
60 min	0.674403	0.606364	0.501812	0.649107	0.625143
-4	0.107872	0.138004	0.161885	0.105946	0.129326
-9	0.133392	0.162741	0.188722	0.118747	0.141363
-11	0.061615	0.078042	0.110205	0.071074	0.075587
-14	0.022718	0.014849	0.037377	0.055127	0.028581
30 min	0.739756	0.812656	0.615289	0.878441	0.79403
-4	0.088052	0.075703	0.134989	0.038313	0.077046
-9	0.113416	0.082678	0.156325	0.043227	0.080864
-11	0.044197	0.027692	0.076541	0.027397	0.03187
-14	0.014579	0.001272	0.016856	0.012622	0.016189
0 min	1	1	1	1	1
-4	0	0	0	0	0
-9	0	0	0	0	0
-11	0	0	0	0	0
-14	0	0	0	0	0



Supplementary Figure 7: The possible mechanism of crosslink (A⁺T) and most abundant thymidine (thymine glycol, 5-HMdUrd, 5-FormdUrd) lesion formations.